AIP | Journal of Applied Physics

# Study of composition dependent structural, optical, and magnetic properties of Cu-doped Zn1−xCdxS nanoparticles

Amit Kumar Chawla, Sonal Singhal, Sandeep Nagar, Hari Om Gupta, and Ramesh Chandra

Citation: J. Appl. Phys. 108, 123519 (2010); doi: 10.1063/1.3524516
View online: http://dx.doi.org/10.1063/1.3524516
View Table of Contents: http://jap.aip.org/resource/1/JAPIAU/v108/i12
Published by the American Institute of Physics.

## Additional information on J. Appl. Phys.

Journal Homepage: http://jap.aip.org/
Journal Information: http://jap.aip.org/about/about_the_journal
Top downloads: http://jap.aip.org/features/most_downloaded
Information for Authors: http://jap.aip.org/authors

ADVERTISEMENT


Downloaded 10 May 2013 to 141.161.91.14. This article is copyrighted as indicated in the abstract. Reuse of AIP content is subject to the terms at: http://jap.aip.org/about/rights_and_permissions

# Study of composition dependent structural, optical, and magnetic properties of Cu-doped $Zn_{1-x}Cd_xS$ nanoparticles

Amit Kumar Chawla,[1] Sonal Singhal,[1,2,3] Sandeep Nagar,[4] Hari Om Gupta,[2] and Ramesh Chandra[1,a)]

[1]*Nanoscience Laboratory, Institute Instrumentation Centre, Indian Institute of Technology Roorkee, Roorkee 247667, India*
[2]*Department of Electrical Engineering, Indian Institute of Technology Roorkee, Roorkee 247667, India*
[3]*Department of Mechanical Material and Manufacturing Engineering, University of Nottingham, NG7 2RD Nottingham, United Kingdom*
[4]*Department of Material Science and Engineering, Royal Institute of Technology, SE-100 44 Stockholm, Sweden*

(Received 17 May 2010; accepted 2 November 2010; published online 28 December 2010)

Cu-doped $Zn_{1-x}Cd_xS$ nanoparticles were synthesized by coprecipitation technique in ice bath at 280 K. The band gap energy of $Zn_{1-x}Cd_xS:Cu$ nanoparticles can be tuned to a lower energy by increasing the Cd content, indicating the formation of the alloyed nanoparticles. The alloy structure is further supported by the systematic shifting of characteristic x-ray diffraction peaks to lower angles with increase in Cd content. Systematic copper doping induces a red shift in the energy band gap of $Zn_{0.9}Cd_{0.1}S:Cu$ nanoparticles with increase in copper concentration. Cu-doped $Zn_{0.9}Cd_{0.1}S$ nanoparticles were found to have ferromagnetic nature at 5 K whereas undoped particles were found to be diamagnetic. Green luminescence further proves proper doping of Cu into the ZnCdS matrix. It is believed that the green luminescence originates from the recombination between the shallow donor level (sulfur vacancy) and the $t_2$ level of $Cu^{2+}$. This method provides an inexpensive and simple procedure to produce ternary ZnCdS:Cu nanoparticles with tunable optical properties via changing Cd and/or Cu concentrations. © *2010 American Institute of Physics*.
[doi:10.1063/1.3524516]

## I. INTRODUCTION

Semiconductor nanoparticles have generated great fundamental and technical interest due to novel size-tunable properties and, consequently, in potential applications as optoelectronic devices and biomedical tags.[1–3] In the past two decades, the main efforts have been focused on the preparation of different color-emitting binary or core-shell nanocrystals with different particle sizes[1,4] using simple and inexpensive chemical routes. However, the tuning of physical and chemical properties by varying the particle size could cause problems in many applications, in particular, if unstable small particles (less than 2 nm) are used.[5] Apart from binary compositions, exploration of tunable optical properties of ternary compositions has become an alternative way to produce desired wavelength by changing their stoichiometries and/or doping.[6] Yang and co-workers reported ternary $Zn_xCd_{1-x}Se$ alloyed nanocrystals with luminescent properties comparable or even better than the best-reported binary CdSe based nanocrystals.[7] We have reported earlier a simple method to manufacture ZnCdS nanoparticles with size tunable properties.[8] Semiconducting nanoparticles, especially sulfides doped with transition metal ions and rare-earth ions, have been studied extensively because of their excellent luminescence properties.[9,10] The optical properties of doped nanomaterials differ from the corresponding host nanomaterials as the dopants form deep trap levels and act as luminescence centers.[11,12] Discrete energy states can be introduced in the band gap of semiconducting host by doping with transition metals such as Cu, Ag and Mn.[13] In this regard, the role of Cu as a luminescence activator is of considerable significance for II-VI compound semiconductors. There have been number of research groups investigating Cu-doped ZnS nanoparticles by chemical routes. Datta *et al.* investigated the effect of Cu incorporation on the phase transition from wrutzite to Cubic structure prepared by solvothermal process.[14] Geng *et al.* have reported the synthesis of $ZnS:Cu^{2+}$ nanorods through a solution phase thermal decomposition molecule precursor route. They were able to tune the optical properties of the products by changing Cu doping concentration.[15] Unni *et al.* synthesize the CdS, $CdS:Zn^{2+}$ and $CdS:Cu^{2+}$ and reported the photoluminescence quenching at 15 wt % of Cu.[16] Bol *et al.* have observed the red emission in addition to the green emission in the PL spectra of Cu doped ZnS nanoparticles.[12] Lowest synthesis temperature considered by other research workers is 300 K. Peng *et al.*[13] have reported the synthesis and photoluminescence properties of Cu doped ZnS nanoparticles via chemical route at 300 K. The highest temperature reported in the literature have gone up to 900–1000 °C. These elevated temperatures are the firing temperature and are applied when nanoparticles found their application in nanophosphor. Nien *et al.*[17] have reported the red electroluminescent phosphor powders synthesized via chemical route and then subjected to the firing temperature of 900 °C. Recently Kim *et al.* have shown the successful formation of transition metal doped $Zn_{1-x}Cd_xS$ nanoparticles at room temperature.[18,19]

a)Electronic mail: ramesfic@iitr.ernet.in.

 © 2010 American Institute of Physics

Downloaded 10 May 2013 to 141.161.91.14. This article is copyrighted as indicated in the abstract. Reuse of AIP content is subject to the terms at: http://jap.aip.org/about/rights_and_permissions

There have been few reports on $Cu^{2+}$ doped $Zn_{1-x}Cd_xS$ nanoparticles[20] at low temperature processing to obtain the green luminescence. To the best of our knowledge, there is no report on the Cu-doped $Zn_{1-x}Cd_xS$ nanoparticles using ice bath synthesis. Thus, herein, we employed chemical route as an aqueous coprecipitation method to synthesize Cu-doped $Zn_{1-x}Cd_xS$ nanoparticles at relatively lower temperature and have explored their composition dependent optical and structural properties.

## II. EXPERIMENT

Cu doped $Zn_{1-x}Cd_xS$ nanoparticles have been synthesized in the laboratory at 280 K using coprecipitation technique in ice bath. Appropriate molar amount of zinc nitrate hexahydrate, cadmium nitrate tetrahydrate, copper nitrate hexahydrate, and sodium sulphide were taken to maintain the stoichiometry of the nanoparticles. In one set of experiment $Zn_{1-x}Cd_xS$ ($x$=0.1, 0.2, 0.3, 0.4, and 0.5) nanoparticles were prepared in a manner that the concentration of Cd is varied such that the mole fraction ($x$), molar ratio of cadmium to zinc, varies in steps of 0.1 from 0.1 to 0.5 while keeping molar amount of copper fixed at 0.005 M. In another experiment, Cd mole fraction ($x$) is kept constant at 0.1 with varying Cu concentrations as 0.005, 0.01, and 0.015 M. In the typical experiment requisite amounts of 0.5 M zinc nitrate, 0.05 M cadmium nitrate and appropriate molar amount of Copper nitrate aqueous solution were mixed. 0.5 M sodium sulfide aqueous solution was added into the above mixture with a dripping speed of ten drops per minute. Continuous stirring was also provided for better intermixing during the length of the reaction at 280 K. The resulting precipitates were filtered off and washed several times in distilled water and acetone. The precipitates were dried in hot air oven at 323 K.

Quantitative elemental analysis was performed by energy dispersive spectrometer attached with FE-SEM (FEI Quanta 200 F). The particle size and the shape of the nanoparticles were determined by transmission electron microscopy (FEI TECNAI-$G^2$). X-ray analysis was performed by using a Diffractometer with Cu $K_\alpha$ target (Bruker D8 Advance) radiation. Optical absorption was measured in the 200–800 nm wavelength range using UV-Vis-NIR spectrophotometer (Cary 5000 Varian). For absorbance measurement the nanoparticles were dispersed in isopropyl alcohol. Isopropyl alcohol has its absorption wavelength at 204 nm and thus it becomes an attractive choice as solvent. In a typical measurement 2 mg of each nanoparticle was dispersed in 50 ml Isopropyl alcohol and the solution was ultrasonicated to prevent the precipitation of sample. A clear solution thus obtained was used for the measurement. For obtaining the absorption characteristics of all the samples, at first the transmittance ($T$) at different wavelengths ($\lambda$) are measured and then absorbance ($\alpha$) at the corresponding wavelengths $\lambda$ are calculated using the Beer–Lambert's relation,

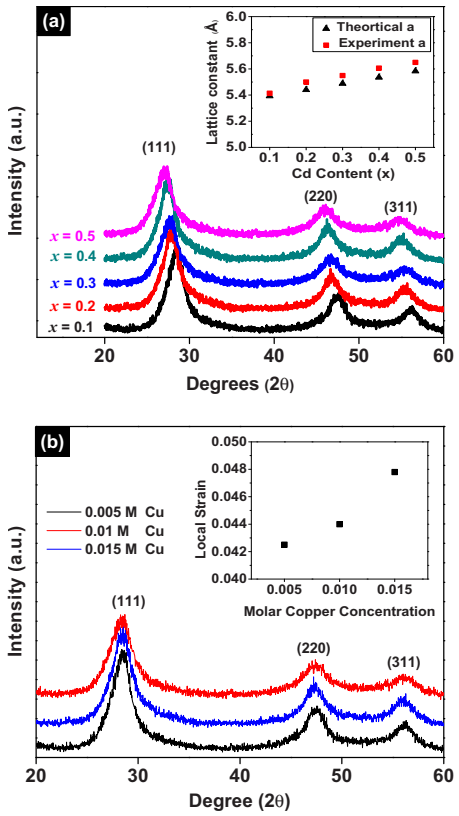


FIG. 1. (Color online) (a) XRD patterns of $Zn_{1-x}Cd_xS$:0.005Cu nanoparticles with $x$=0.1, 0.2, 0.3, 0.4, and 0.5. Inset shows the lattice constants of $Zn_{1-x}Cd_xS$:0.005Cu nanoparticles in cubic structure (b) XRD patterns of Cu-doped $Zn_{0.9}Cd_{0.1}S$ nanoparticles with Cu concentrations of 0.005, 0.01, and 0.015 M. Inset shows the local strain values with varying Cu concentrations.

$$\alpha = \frac{1}{d}\ln\left(\frac{1}{T}\right),$$

where $d$ is the path length in centimeter. In our case the path length considered was 1 cm. Photoluminescence emission spectra were recorded at room temperature with a photoluminescence spectrometer (Perkins Elmer LS 55). Magnetic measurements were taken with superconducting quantum interference device (SQUID) magnetometer (QD MPMS-XL).

## III. RESULTS AND DISCUSSIONS

Figure 1(a) shows the XRD (X-Ray Diffraction) patterns of nanoparticles for different mole fractions ($x$) with Cu concentration of 0.005 M. All the samples obtained under the present synthesis conditions exhibited a cubic structure with broad diffraction peaks of (111), (220), and (311) orientations. No peaks for any impurity phase or metallic clustering was observed. It can be seen from Fig. 1(a) that the XRD peaks shifts to lower angles gradually with increase in mole fraction. This shift toward lower angle is believed to result from the incorporation of Cd ions into the ZnS lattice.[8] Continuous peak shifting of the nanoparticles suggest a successful formation of alloyed nanoparticles. We also calculate the average crystallite size from the XRD peak broadening by using Scherrer formula, ($d$=0.9$\lambda$/$\beta$ cos $\theta$), where $d$ is the particle size in angstroms, $\beta$ is the full width at half maxi-

Downloaded 10 May 2013 to 141.161.91.14. This article is copyrighted as indicated in the abstract. Reuse of AIP content is subject to the terms at: http://jap.aip.org/about/rights_and_permissions

mum (FWHM), λ is the wavelength of the x-rays used (=1.54 Å).[21] Particle sizes of 3.80 nm, 3.76 nm, 3.71 nm, 3.67 nm, and 3.65 nm have been obtained for the mole fraction, $x$ of 0.1, 0.2, 0.3, 0.4, and 0.5, respectively.

Semiconductor alloys (solid solutions) have been proposed to obey Vegard's law,[22] revealing the linear relationship between the lattice constant and composition as follows:

$$a^0_{A_{1-x}B_xC}(x) = (1-x)a^0_{AC} + xa^0_{BC}, \quad (1)$$

where $a^0_{A_{1-x}B_xC}$ is the natural constant of the ternary form $A_{1-x}B_xC$ and $a^0_{AC}$ and $a^0_{BC}$ are the natural constants of the binaries AC and BC, respectively, and $x$ is the mole fraction of binary BC ranging from 0 to 1. In the case of Cubic $Zn_{1-x}Cd_xS$ nanoparticles, the ideal lattice constant with Cd concentration of 0.05 M is 5.392 Å, where cubic $a^0_{ZnS}$ =5.345 Å (PDF # 80–0020) and $a^0_{CdS}$=5.820 Å (PDF # 01–0647). Square data points in the inset of Fig. 1(a) correspond to lattice constants of $Zn_{1-x}Cd_xS$ with mole fractions in cubic structure obtained from XRD data. The triangular data points are obtained by Vegard's law using Eq. (1). Vegard's law was applied to check the compositional homogeneity of the semiconductor nanoparticles. It can be seen from the inset of Fig. 1(a) that there is a gradual increase in the lattice parameter with increase in the mole fraction. This trend is consistent with Vegard's law and indicates a homogeneous alloy structure. The close agreement between the experimental and the theoretical lattice values also indicates that the composition of the nanoparticles was very close to the mixing molar ratio of the starting materials of ZnS and CdS and it rules out the possibility of a separate nucleation of CdS and ZnS.

Figure 1(b) shows the XRD patterns of the $Zn_{0.9}Cd_{0.1}S$ nanoparticles with Cu concentrations of 0.005, 0.01, and 0.015 M. Cubic structure with (111), (220), and (311) orientations were obtained. The average crystallite size came out to be 3.8, 3.6, and 3.5 nm for Cu-doped $Zn_{0.9}Cd_{0.1}S$ nanoparticles with Cu concentrations of 0.005, 0.01, and 0.015 M, respectively. It can be seen from Fig. 1(b) that there is a slight shift in the XRD peak position toward lower angle with increase in Cu concentration. A shift in the d spacing is attributed to the strain produced in the lattice upon Cu incorporation. Resulting strain in the lattice arises due to the differences in the ionic radii of $Zn^{2+}$ (0.74 Å) and $Cu^{2+}$ (0.72 Å).[23] According to Hume Rothary rules for the formation of substitutional solid solutions, the ionic radii of the solute and solvent atoms must differ by no more than 15%. In the present case ionic radii difference is came to be around ~2.7% which is fairly smaller than 15%, satisfying the Hume–Rothary rule.[24] This helps to rule out the possibility of "Cu" ions coming out of the host lattice. Thus, one can clearly conclude that substitutional Cu-doping in $Zn_{1-x}Cd_xS$ lattice is accomplished. In order to find out the extent of strain that have been induced in the lattice due to copper incorporation, strain analysis has also been carried out. Local strain is calculated by making use of Scherrer formula of $\Delta k$ versus $k$ [the scattering vector $k=(4\pi/\lambda)\sin\theta$].[25] The three peaks of (111), (220), and (311) were fitted linearly to obtain the local strain values. Calculated values of local strain are shown in the inset of Fig. 1(b). Local strain increases, as expected, with increase in the copper concentration.

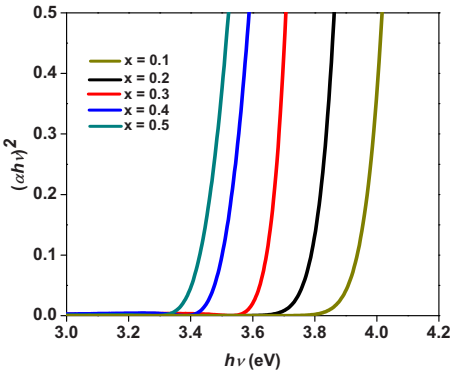


FIG. 2. (Color online) $(\alpha h\nu)^2$ vs photon energy of $Zn_{1-x}Cd_xS$:0.005Cu nanoparticles with $x$=0.1, 0.2, 0.3, 0.4, and 0.5.

Figure 2 shows the $(\alpha h\nu)^2$ versus photon energy of $Zn_{1-x}Cd_xS$:0.005Cu nanoparticles with the mole fraction. The red-shift in band gap from 3.95 to 3.43 eV with increasing mole fraction clearly indicates the formation of alloyed nanoparticles also supporting the XRD data. We also developed an equation with the input values as the experimental band gap values obtained by absorption measurement. Figure 3 shows the fit to the energy band gap values. Regression coefficient is found close to 1, signifies that the trend line fits very well to the experimental data points.

$$E_g(x) = 4.17 - 2.34x + 1.73x^2; \quad R^2 = 0.998. \quad (2)$$

Bowing parameter is the coefficient of the quadratic term of the above equation and has a value of 1.73.

In bulk CdS–ZnS alloyed crystals their composition ($x$) dependent bandgap energies $[E_g(x)]$ can be expressed by the relation[22]

$$E_g(x) = E_g(\mathrm{ZnS}) + [E_g(\mathrm{CdS}) - E_g(\mathrm{ZnS}) - b]x + bx^2, \quad (3)$$

where $E_g$(ZnS) and $E_g$(CdS) are the band gap energies for bulk ZnS ($E_g$=3.6 eV) and CdS ($E_g$=2.36 eV), respectively, and $b$ is the bowing parameter (bulk value for bowing parameter is 0.61).[26,27]

In Fig. 4 calculated results for alloyed bulks [using Eq. (3)] and nanoparticles [using Eq. (2)] are shown as the dotted and solid lines, respectively. Using the calculated bandgap energy (line curve) of $Zn_{1-x}Cd_xS$:0.005Cu nanoparticles, the actual compositions of $Zn_{1-x}Cd_xS$:0.005Cu nanoparticles can be indirectly estimated. EDS results shows that the mole

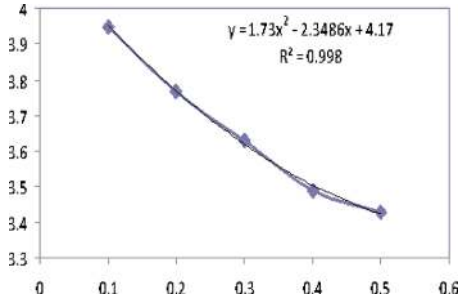


FIG. 3. (Color online) A polynomial fit to to the energy band gap values obtained from absorbance nmeasurement.

Downloaded 10 May 2013 to 141.161.91.14. This article is copyrighted as indicated in the abstract. Reuse of AIP content is subject to the terms at: http://jap.aip.org/about/rights_and_permissions

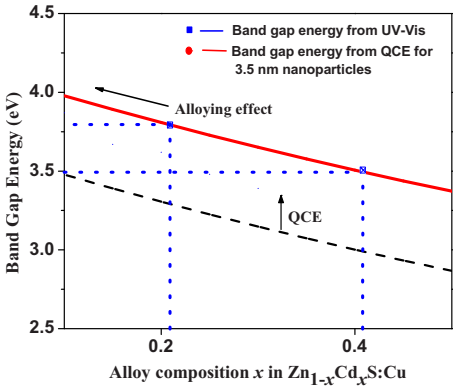


FIG. 4. (Color online) Alloy composition dependence of calculated absorption energies of bulk crystals (dashed lines) and nanoparticles (solid line). Dashed line is obtained by using Eq. (3) by taking the bulk energy band gap values for ZnS and CdS. Solid line is obtained by making use of Eq. (4). The shift to a higher energy from the dashed to solid line is due to the QCE.

fraction $(x)$ of $0.11 \pm 0.045$, $0.22 \pm 0.038$, $0.31 \pm 0.051$, $0.41 \pm 0.048$, $0.52 \pm 0.049$ are obtained for 0.1, 0.2, 0.3, 0.4, and 0.5, respectively.

Figure 5(a) shows the absorption spectra of Cu-doped $Zn_{0.9}Cd_{0.1}S$ nanoparticles with Cu concentrations of 0.005, 0.01, and 0.015 M. Figure 5(b) shows the plot of $(\alpha h\nu)^2$ against the photon energy $(h\nu)$ with variation ion Cu concentration. The direct band gap of these nanoparticles was determined by taking an extrapolation of the linear region of a plot of $(\alpha h\nu)^2$. In order to investigate the effect of quantum confinement in the Cu-doped $Zn_{0.9}Cd_{0.1}S$ nanoparticles a comparison is made with respect to the undoped nanoparticles. For undoped $Zn_{0.9}Cd_{0.1}S$ nanoparticles with particle

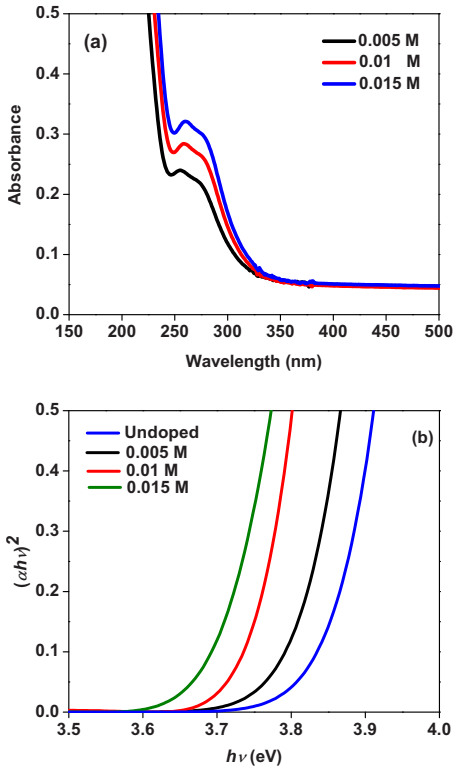


FIG. 5. (Color online) $Zn_{0.9}Cd_{0.1}S$ nanoparticles with Cu concentrations of 0.005, 0.01, and 0.015 M (a) Absorption spectra (b) $(\alpha h\nu)^2$ vs $h\nu$ plots.

TABLE I. Cu molar concentrations in starting solution and analyzed from EDS, average particle size, local strain, lattice constant as obtained by XRD, and energy band gap as determined by UV-Vis measurements.

| Cu in starting solution (M) | Cu concentration determined by EDS (M) | $d_{XRD}$ (nm) | Local strain | Lattice constant (Å) | Band gap (eV) |
|---|---|---|---|---|---|
| 0.005 | 0.0041 | 3.8 | 0.0425 | 5.410 | 3.78 |
| 0.010 | 0.0073 | 3.6 | 0.0442 | 5.389 | 3.73 |
| 0.015 | 0.0109 | 3.5 | 0.0471 | 5.384 | 3.69 |

size of 3.5 nm, energy band gap can be calculated by using Eq. (3). Brus showed that semiconductor nanoparticles with a particle radius significantly smaller than the exciton Bohr radius exhibit strong size-dependent optical properties due to the strong quantum confinement effect (QCE),[28]

$$E_g = E_g^0 + \frac{h^2}{8\mu R^2} - \frac{1.8e^2}{4\pi\varepsilon R}. \quad (4)$$

Where $E_g^0$ is the energy band gap for the bulk material, $R$ is the radius of the nanoparticle calculated from XRD data, $1/\mu = 1/m_e + 1/m_h$ ($m_e$ and $m_h$ being the electron and hole effective masses, respectively), $\varepsilon$ is the dielectric constant and $e$ is the electronic charge. Here the electron effective mass $(m_e)$, hole effective mass $(m_h)$, and dielectric constant $(\varepsilon)$ for ZnS are $0.25m_o$, $0.51m_o$, and $5.2\varepsilon_0$, respectively.[29]

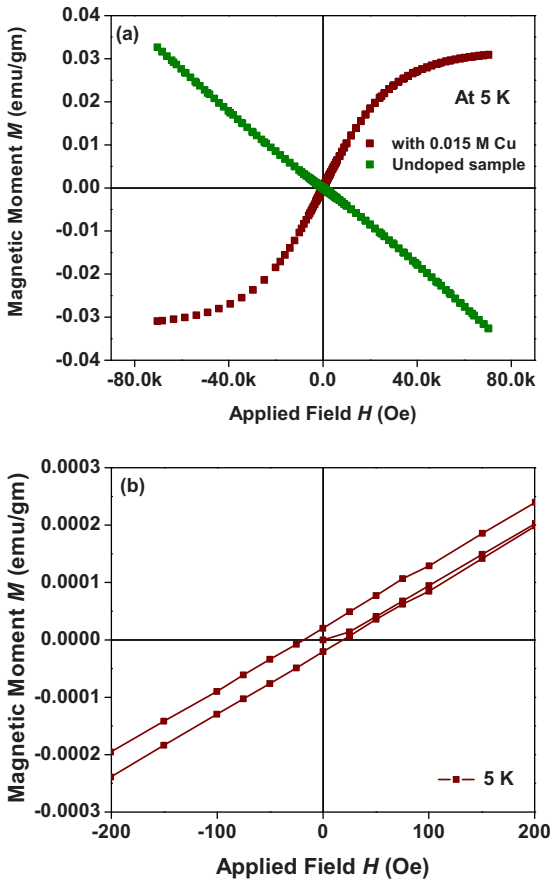


FIG. 6. (Color online) (a) Magnetization vs applied magnetic field of 0.015 M Cu–doped and undoped nanoparticles at temperature of 5 K (b) Low field region of 0.015 M Cu nanoparticles.

Downloaded 10 May 2013 to 141.161.91.14. This article is copyrighted as indicated in the abstract. Reuse of AIP content is subject to the terms at: http://jap.aip.org/about/rights_and_permissions

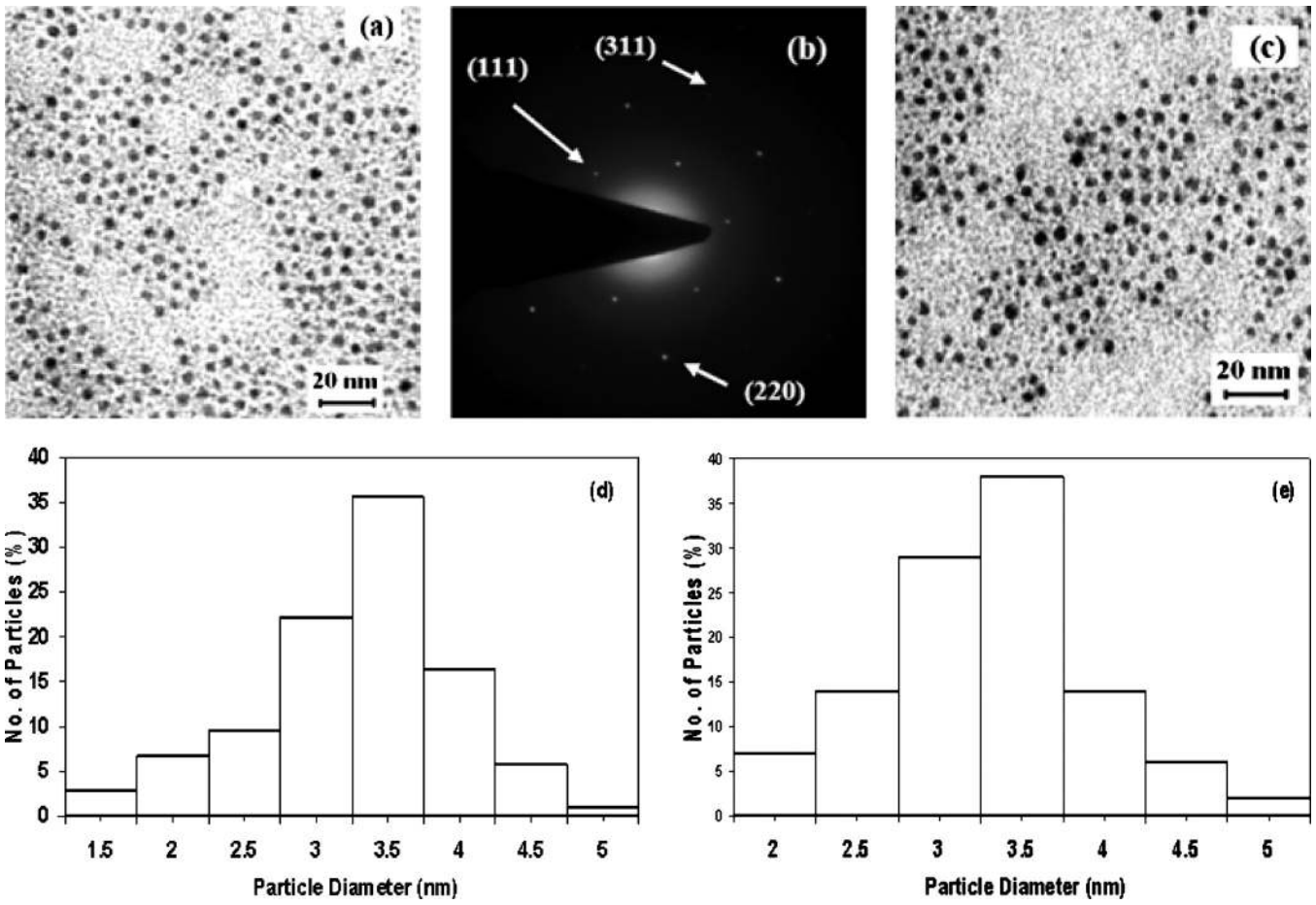


FIG. 7. (a) TEM image of $Zn_{0.9}Cd_{0.1}S:0.005Cu$ nanoparticles (b) Corresponding SAED pattern showing cubic structure. (c) TEM image of $Zn_{0.9}Cd_{0.1}S:0.015Cu$ nanoparticles (d) Size distribution histogram of $Zn_{0.9}Cd_{0.1}S:0.005Cu$ nanoparticles (e) Size distribution histogram of $Zn_{0.9}Cd_{0.1}S:0.015Cu$ nanoparticles.

Corresponding values for CdS are $0.19m_o$, $0.8m_o$, and $5.7\varepsilon_0$.[29] By substituting these values in Eq. (4), size dependent band gap energy value of 4.005 eV and 2.97 eV for ZnS and CdS, respectively, are obtained. Therefore, now making use of Eq. (3) the composition ($x$) dependent band gap energy of 3.84 eV is obtained for undoped $Zn_{0.9}Cd_{0.1}S$ alloyed nanoparticles. The band gap for undoped sample ($E_g$ =3.82 eV) obtained from UV-Vis measurements was in agreement with the composition dependent quantum confined energy band gap ($E_g$=3.84 eV). The direct energy band gap of 3.78 eV, 3.73 eV, and 3.69 eV corresponding to Copper concentrations of 0.005 M, 0.01 M, and 0.015 M, respectively, is obtained. It is worthy to note that there is a gradual red shift in the energy band gap of $Zn_{0.9}Cd_{0.1}S:Cu$ nanoparticles with increase in copper concentration.

EDS measurements revealed that the Cu concentration in the nanoparticles is less compared to their respective amount added in the reaction. Cu concentration, as determined by EDS, is shown in Table I. We believe that some factors which cannot be controlled precisely, stirring speed and the mixture process of the solution, are responsible for discrepancy in the Cu content. In addition to the EDS measurement we have taken the SQUID measurements of Cu-doped nanoparticles in order to probe the ability to dope $Cu^{2+}$ in the $Zn_{0.9}Cd_{0.1}S$ nanoparticles. Figure 6(a) shows the field dependent magnetization ($M$-$H$) curves of nanoparticles with 0.015 M Cu at 5 K. For the sake of comparison $M$-$H$ measurements of undoped sample was also taken at 5 K and is shown in the same figure. From the M-H measurements it is clear that at 5 K, the doped sample shows ferromagnetism while the undoped exhibits, as expected, a diamagnetic behavior. Figure 6(b) shows the low-field region of the loop, showing coercivity ($H_C$) of ~20 Oe and remanent magnetization (Mr) of $\sim 2.14 \times 10^{-5}$ emu/gm for 0.015 M Cu doped $Zn_{0.9}Cd_{0.1}S$ nanoparticles.

TEM (Transmission Electron Microscope) measurements were also performed to confirm the nanocrystalline nature and to study the morphology of the particles. Typical TEM micrographs of $Zn_{0.9}Cd_{0.1}S:0.005Cu$ and $Zn_{0.9}Cd_{0.1}S:0.015Cu$ nanoparticles are shown in Figs. 7(a) and 7(c). The particles in samples are found to be nearly spherical in shape. Particle size distribution is also obtained by the TEM images. As-prepared $Zn_{0.9}Cd_{0.1}S:Cu$ nanoparticles with corresponding Cu concentrations of 0.005 and 0.015 M, have narrow size distributions with a relative standard deviation of 12%–15% and 15%–18%, respectively, without any size sorting (refer to the size distribution histograms of nanoparticles with 0.005 and 0.015 M Cu concentration in Figs. 7(d) and 7(e), respectively). Figure 7(b) shows the selected area electron diffraction (SAED) pattern

Downloaded 10 May 2013 to 141.161.91.14. This article is copyrighted as indicated in the abstract. Reuse of AIP content is subject to the terms at: http://jap.aip.org/about/rights_and_permissions

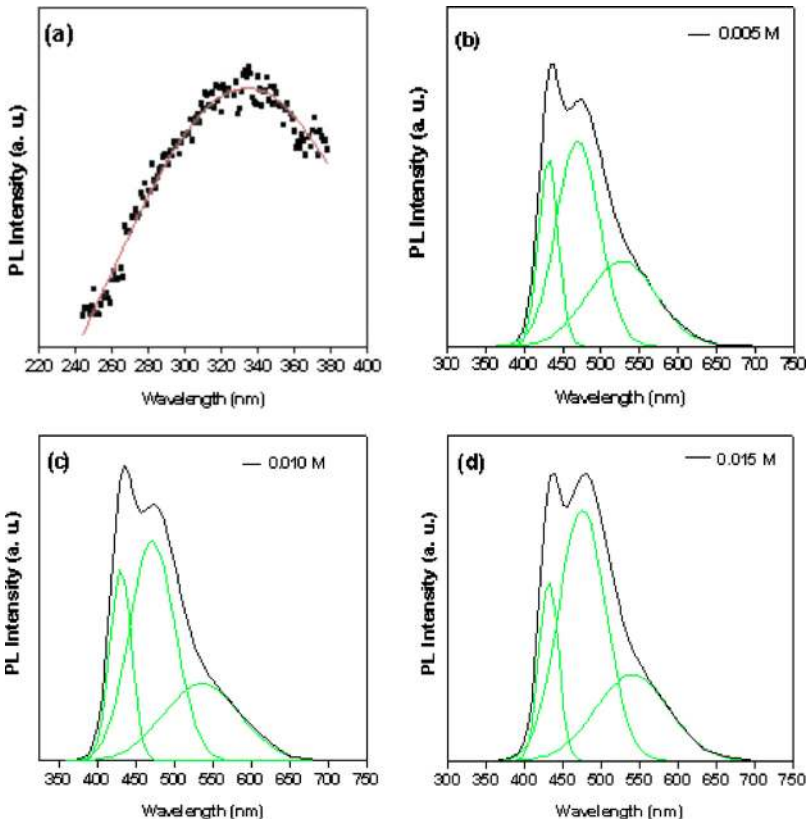


FIG. 8. (Color online) Room temperature photoluminescence spectra (a) Excitation spectra of $Zn_{0.9}Cd_{0.1}S$ nanoparticles with Cu doping of 0.005 M. Emission spectra of $Zn_{0.9}Cd_{0.1}S$ nanoparticles with Cu concentration of (b) 0.005 M (c) 0.01 M, and (d) 0.015 M respectively.

of $Zn_{0.9}Cd_{0.1}S$ nanoparticles with characteristic of a cubic phase. In Fig. 7(b) the first ring indicates a periodical structure with length of 3.1 Å, which is coincident with the standard cubic $Zn_{0.9}Cd_{0.1}S$ interplanar distance of 3.126 Å in the (111) direction, and is essentially the same as that obtained by Vegard's law.[22] We also believe that there is no signature of CuS or other impurity phases in our samples. XRD does not show any detectable signal of Cu or CuS, which means that the content of CuS or Cu in the samples is at most less than 5% (5% is the detection limit of XRD). TEM diffraction pattern also support our argument as, we did not find any other diffraction rings in our TEM diffraction pattern that cannot be indexed by sphalerite structure. Also the undoped nanoparticles show the diamagnetic behavior and the Cu doped $Zn_{0.9}Cd_{0.1}S$ nanoparticle shows the ferromagnetic behavior at temperature down to 5 K. This eliminates the possibility of the existence of CuS or other impurity phases in the samples.

The room temperature PL excitation and emission spectra of $Zn_{0.9}Cd_{0.1}S$ nanoparticles with Cu concentrations of 0.005, 0.01, and 0.015 M are shown in Fig. 8. Figure 8(a) shows the PLE spectra of 0.01 M Cu-doped nanoparticles for the PL emission of 537 nm. The experimental data is shown as solid squares. The solid line shows the Gaussian fitting on this data ($R^2$=0.96). Gaussian fitting provides the mean value at 335 nm. Nanoparticles with 0.005 and 0.015 M also showed peak at 335 nm. All PL emission spectra were therefore recorded at an excitation wavelength of 335 nm. Broad and asymmetric spectrum suggests that these are the superposition of emission peaks. A Gaussian curve fitting was used to deconvolute the PL curves. All the PL emission spectrums have been deconvoluted into three mains peaks and the results are given in Table II.

The room temperature PL emission spectra of $Zn_{0.9}Cd_{0.1}S$ nanoparticles with Cu concentrations of 0.005, 0.01, and 0.015 M are shown in Figs. 8(b)–8(d). The 431 nm emission (peak I) has been classically termed as self activated luminescence and known to be due to recombination of carriers between sulfur vacancy ($V_s$) related donor level and the valance band edge.[30] As shown in Table I the peak position of this emission does not change with the increase in Cu concentration. Similar result has also been reported by Peng. *et al.*[13] where they attribute it to the constant energy level of sulfur vacancy with respect to the valance band. The ~470 nm blue emission (peak II) is attributed to recombination from the conduction band edge to zinc/cadmium vacancy ($V_{zn}/V_{cd}$) related acceptor level.[30] No appreciable shift in peak position is noticed with increase in Cu content. PL spectra also consist of the green emission. The green emission is attributed to transition between sulfur vacancy ($V_s$) related donor level and the additional "$t_2$" levels of Cu doping which acted as the luminescence centers.[31] With increase in the $Cu^{2+}$ concentration, the green emission (peak III) systematically shifts to longer wavelength (from 526 to

TABLE II. Photoluminescence peak position in the $Zn_{0.9}Cd_{0.1}S$ nanoparticles with varying Cu concentration.

| Cu concentration (M) | PL peak positions (nm) | | |
|---|---|---|---|
| | Peak I | Peak II | Peak III |
| 0.005 | 431 | 469 | 526 |
| 0.010 | 431 | 471 | 535 |
| 0.015 | 430 | 473 | 540 |

Downloaded 10 May 2013 to 141.161.91.14. This article is copyrighted as indicated in the abstract. Reuse of AIP content is subject to the terms at: http://jap.aip.org/about/rights_and_permissions

540 nm). This shift in green emission is due to increased incorporation of Cu ions into $Zn_{0.9}Cd_{0.1}S$ nanoparticles.

## IV. CONCLUSIONS

The low temperature coprecipitation technique results in the successful synthesis of cubic structured Cu-doped $Zn_{1-x}Cd_xS$ nanoparticles with controllable compositions and very small sizes of around 3.5 nm. With increase in the Cd content, keeping Cu fixed at 0.005 M, absorption spectra red-shifts systematically, indicating the formation of the alloyed nanoparticles. A decrease in band gap with increase in copper concentration in $Zn_{0.9}Cd_{0.1}S$ is also observed. TEM diffraction pattern confirms X-ray diffraction predictions about size and crystallinity of copper doped $Zn_{0.9}Cd_{0.1}S$ nanoparticles. The magnetic measurement shows that the Cu doped $Zn_{0.9}Cd_{0.1}S$ nanoparticles are ferromagnetic in nature with coercivity ($H_C$) of ~20 Oe and remanent magnetization ($Mr$) of $\sim 2.14 \times 10^{-5}$ emu/gm for 0.015 M Cu doped $Zn_{0.9}Cd_{0.1}S$ nanoparticles. No signature of CuS or other impurity phases are found in our samples. With increase in the $Cu^{2+}$ concentration, the green emission peak, attributed to the recombination between the shallow donor level (sulfur vacancy) and the $t_2$ level of $Cu^{2+}$, systematically shifts from 526 to 540 nm. This method can be used to synthesize small sized doped and undoped ZnCdS nanoparticles with tunable optical properties by varying either the constituents of host or the concentration of dopant.

## ACKNOWLEDGMENTS

We are grateful to Dr. A. C. Pandey, Director, Nanophospher Application Centre, Allahabad for providing the photoluminescence facility.

[1]S. J. Pearton, D. P. Norton, K. Ip, Y. W. Heo, and T. Steiner, J. Vac. Sci. Technol. **22**, 932 (2004).
[2]A. H. MacDonald, P. Shiffer, and N. Samarth, Nature Mater. **4**, 195 (2005).
[3]H. Ohno, Science **281**, 951 (1998).
[4]D. Jiang, L. Cao, G. Su, W. Liu, H. Qu, Y. Sun, and B. Dong, J. Mater. Sci. **44**, 2792 (2009).
[5]X. Zhong and Y. Feng, Res. Chem. Intermed. **34**, 287 (2008).
[6]R. Sethi, L. Kumar, and A. C. Pandey, J. Nanosci. Nanotechnol. **9**, 5329 (2009).
[7]Y. M. Sung, Y. J. Lee, and K. S. Park, J. Am. Chem. Soc. **128**, 9002 (2006).
[8]S. Singhal, A. K. Chawla, S. Nagar, H. O. Gupta, and R. Chandra, J. Nanopart. Res. **12**, 1415 (2010).
[9]A. A. Khosravi, M. Kundu, L. Jatwa, S. K. Deshpanee, U. A. Bhagwat, M. Sastri, and S. K. Kulkarni, Appl. Phys. Lett. **67**, 2702 (1995).
[10]B. Y. Geng, L. D. Zhang, G. Z. Wang, T. Xie, Y. G. Zhang, and G. W. Meng, Appl. Phys. Lett. **84**, 2157 (2004).
[11]S. J. Xu, S. J. Chua, B. Liu, L. M. Gan, C. H. Chew, and G. Q. Xu, Appl. Phys. Lett. **73**, 478 (1998).
[12]A. A. Bol, J. Ferwerda, J. A. Bergwerff, and A. Meijerink, J. Lumin. **99**, 325 (2002).
[13]W. Q. Peng, G. W. Cong., S. C. Qu, and Z. G. Wang, Opt. Mater. **29**, 313 (2006).
[14]A. Dutta, S. K. Panda, and S. Chaudhuri, J. Solid State Chem. **181**, 2332 (2008).
[15]B. Geng, J. Ma, and F. Zhan, Mater. Chem. Phys. **113**, 534 (2009).
[16]C. Unni, D. Philip, S. L. Smitha, K. M. Nissamudeen, and K. G. Gopchandran, Spectrochim. Acta, Part A **72**, 827 (2009).
[17]Y. T. Nien, P.W. Chen, and I. G. Chen, J. Alloys Compd. **462**, 398 (2008).
[18]T. Y. Lui, J. A. Zapien, H. Tang, D. D. D. Ma, Y. K. Liu, C. S. Lee, S. T. Lee, S. L. Shi, and S. J. Xu, Nanotechnology **17**, 5935 (2006).
[19]J. U. Kim, Y. K. Kim, and H. Yang, J. Colloid Interface Sci. **59**, 341 (2010).
[20]J. U. Kim, M. H. Lee, and H. Yang, Nanotechnology **19**, 465605 (2008).
[21]B. D. Cullity and S. R. Stock, in *Elements of X-Ray Diffraction*, 3rd ed., edited by P. Hall (Prentice Hall, New Jersey, 2001), p. 170.
[22]J. Singh, *Optoelectronics An Introduction to Materials and Devices* (McGraw-Hill, New York, 1996).
[23]L. Q. Yan, F. Macia, Z.-W. Jiang, J. Shen, L.-H. He, and F. W. Wang, J. Phys.: Condens. Matter **20**, 255203 (2008).
[24]A. P. Tsai, J. Non-Cryst. Solids **334–335**, 317 (2004).
[25]D. Son, D. R. Jung, J. Kim, T. Moon, C. Kim, and B. Park, Appl. Phys. Lett. **90**, 101910 (2007).
[26]S. M. Sze, *Physics of Semiconductor Devices* (Wiley, New York, 1969).
[27]A. Goudarzi, G. M. Aval, R. Sahrai, and H. Ahmadpoor, Thin Solid Films **516**, 4953 (2008).
[28]L. E. Brus, J. Chem. Phys. **80**, 4403 (1984).
[29]H. Ohde, M. Ohde, F. Bailey, H. Kim, and C. M. Wai, Nano Lett. **2**, 721 (2002).
[30]K. Jayanthi, S. Chawla, H. Chander, and D. Haranath, Cryst. Res. Technol. **42**, 976 (2007).
[31]A. Dutta, S. Biswas, S. Kar, and S. Chaudhuri, J. Nanosci. Nanotechnol. **7**, 3670 (2007).

Downloaded 10 May 2013 to 141.161.91.14. This article is copyrighted as indicated in the abstract. Reuse of AIP content is subject to the terms at: http://jap.aip.org/about/rights_and_permissions